



Research paper

A study on the deflection and crack layout in a hollow slab bridge

Songtao Wang¹, Dawei Wang²

Abstract: This paper conducts research based on the hollow slab members in the reconstruction and expansion project of expressways, two types of numerical finite element models with and without considering bond-slip relationship of reinforcement and concrete are established, and verified by tests. The distribution characteristics of crack spacing in reinforced concrete beams are studied. The results show that the bond-slip characteristics of reinforced concrete have little effect on the load-deflection characteristics of 8m hollow slab beam. Due to the influence of the bond-slip relationship of reinforced concrete, the load-deflection curve is partially serrated, while without considering the bond-slip relationship of reinforced concrete, the load-deflection curve is smooth. In the numerical model without considering the bond-slip characteristics, almost all damage occurs in the longitudinal direction, and the distribution characteristics of cracks can't be accurately determined. Regardless of whether the bond-slip is considered or not, the macroscopic characteristics of the stress distribution is: smaller near the support and larger at the mid-span. As secondary flexural cracks expand, models with and without consideration of bond-slip characteristics can't calculate crack spacing based on the stress distribution characteristics of the reinforcement.

Keywords: bridge engineering, hollow slab beam, bond-slip, crack spacing, reinforcement stress

¹M.A., Shandong High-speed Group Co., Ltd., No.0, Longding Road, Jinan, China, e-mail: 823499748@qq.com, ORCID: [0000-0002-3935-0679](https://orcid.org/0000-0002-3935-0679)

²M.A., Geotechnical and Structural Engineering Research Center of Shandong University, 17923 Jingshi Road, Jinan, China, e-mail: 373595817@qq.com, ORCID: [0000-0003-0803-9391](https://orcid.org/0000-0003-0803-9391)

1. Introduction

There are many reasons for the concrete cracking, which will affect the safety of bridge engineering, resulting in the stiffness and the durability of bridge structure reduced. Therefore, both the bridge code [1] and the concrete structure design code [2] have made detailed provisions on the crack checking calculation. Lateral cracks of members caused by tensile and bending moments under load are one of the most common macro-bending cracks. The specifications [2] have put forward specific crack control requirements and are used as one of the checking contents of the serviceability limit.

Most of the existing studies are based on the experimental test [3] or theoretical analysis to study the crack characteristics of reinforced concrete beams [4]. There are three basic theories in the research of reinforced concrete beams: bond-slip theory, no slip theory and comprehensive crack theory. Among them, bond-slip theory is the most classical and widely used. Creazza [5] based on bond-slip theory, established a new model for predicting crack width of different reinforcement ratios and concrete strength classes. Oh [6] modeled the bond stress-slip relationship and the variation of transfer length between reinforcement and concrete under repeated loading, proposed a method to accurately predict the crack width of reinforced concrete beam under repeated loading. Kwak [7] modified the bond stress-slip relationship of reinforced concrete, proposed an numerical model which can analyse the post-cracking behavior and tension stiffening effect in a reinforced concrete tension member. The description of cracks in European and American codes is also based on the theory of bond-slip [8]. According to the bond-slip theory, the stress of reinforcement is transmitted to concrete through the bond stress between reinforcement and concrete, inconsistent deformation causes cracks to develop. The theory of no slip assumes that there is no relative slip between the steel bar and the concrete along the horizontal plane. The crack width at the steel bar should be zero, the crack development shape is wedge-shaped, and the crack width at the edge of the concrete is the widest. The main reason of crack formation is the deformation of concrete around the reinforcement. The bond-slip theory and no slip theory are considered in the comprehensive crack theory. However, the existing research shows that [9]: the calculation results of cracks established by various theories are quite different. The crack theory of reinforced concrete needs further research. Subsequent research needs to develop more reasonable cracking tests and adopt more accurate numerical models to simulate and analyze, so as to establish a recognized cracking theory of reinforced concrete.

The nonlinear finite element analysis method can simulate the stress characteristics of reinforced concrete beams from cracking to failure. Casanova [10] established a bond-slip model of reinforced concrete by finite element method, studied the characteristic stress distribution related to the transfer of bond force from steel to concrete. However, there are relatively few researches on how to obtain more accurate crack distribution characteristics using numerical finite element analysis. There have been a few studies based on extended finite element [11] to study the crack distribution characteristics of reinforced concrete members.

At present, there are few researches on the details of cracks in reinforced concrete beams based on numerical analysis methods, and it is rarer to carry out similar studies

on the beams of actual bridges [11]. In this paper, the actual hollow slab members in an expressway reconstruction and expansion project are taken as the research object. The crack distribution characteristics are obtained through testing. A refined numerical finite element model is established to study the distribution characteristics of crack spacing in reinforced concrete.

2. Test program

2.1. Introduction to hollow slab model

An internal slab of a hollow slab bridge with a span of 8 m was selected as the test object and the cross-section of the test slab is shown in Figure 1. The original pavement of the bridge was 10 cm thick concrete. Around 2006, the bridge management department upgraded the bridge deck pavement by removing the asphalt layer and adding a 7 cm thick concrete layer. 8 ribbed steel bars with a diameter of 25 mm is arranged in the hollow slab. C40 concrete is used in the concrete leveling layer, hollow slabs and hinges, and the Q335 steel bars are selected (Table 1).

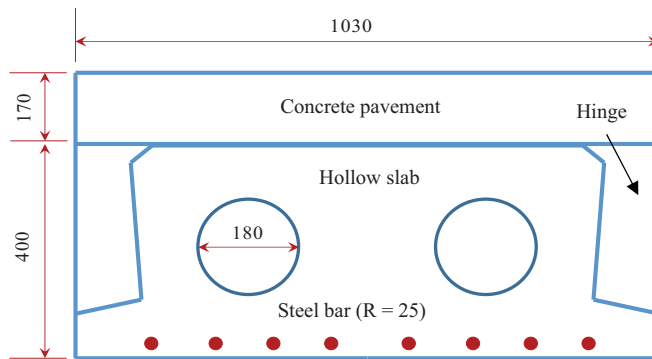


Fig. 1. Cross section of hollow slab (units: mm)

Table 1. Mechanical properties of test hollow slab materials

Material	Mechanical properties			
	Compressive strength (MPa)	Yield strength (MPa)	Tensile strength (MPa)	Elastic modulus (MPa)
C40	26.8	–	2.39	32500
Q335	–	335	370	2100000

For concrete, the compressive and tensile strength refers to the standard value of axial compressive and tensile strength, respectively.

2.2. Load program

The loading scheme of the hollow slab failure test is shown in Figure 2. The loading device consists of a hydraulic system combined with a reaction frame to provide vertical concentrated force for symmetrical loading at two points across the center. The center distance between loading points is 2.0 m. In the early loading, a relatively large load step is used, and the load step is reduced when the elastoplastic turning point is approached.

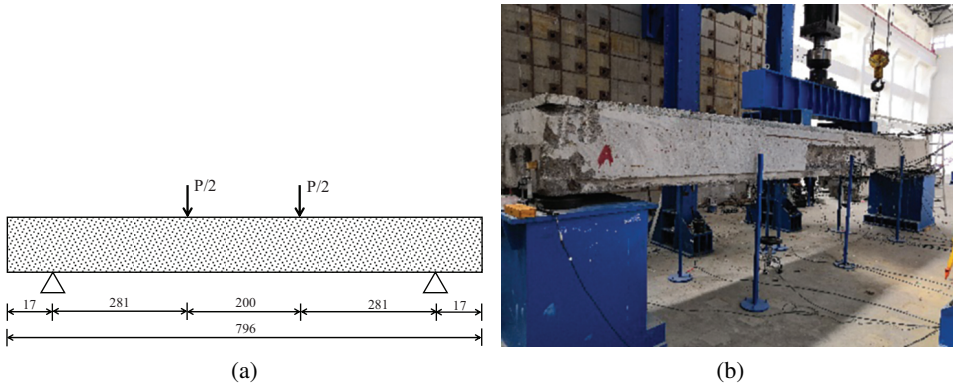


Fig. 2. Loading scheme. (a) Description schematic diagram (units: mm); (b) Photo of the slab

3. Numerical simulation

3.1. Constitutive models of steel bar and concrete

The numerical simulation uses ABAQUS software [12], a plastic damage model is used to simulated concrete. This model assumes that tensile and compression are the main causes of material failure, and describes the inelastic deformation behavior of the material in the form of isotropic elastic damage combined with isotropic tensile and compression plasticity. The evolution of the yield or failure surface are decided by the tensile equivalent plastic strain $\bar{\varepsilon}_t^{pl}$ and compressive equivalent plastic strain $\bar{\varepsilon}_c^{pl}$. Figure 3 and Figure 4 show the stress-strain diagram of concrete under uniaxial tension and compression, respectively. It can be seen that in the elastic stage of the material, a linear elastic constitutive relation is adopted to describe the mechanical properties of the material while in the damage stage, the damage factor d is used to modify the non-destructive initial elastic modulus [12]:

$$(3.1) \quad E = (1 - d)E_0$$

where E_0 is the non-destructive initial elastic modulus of the material, and d is the damage factor.

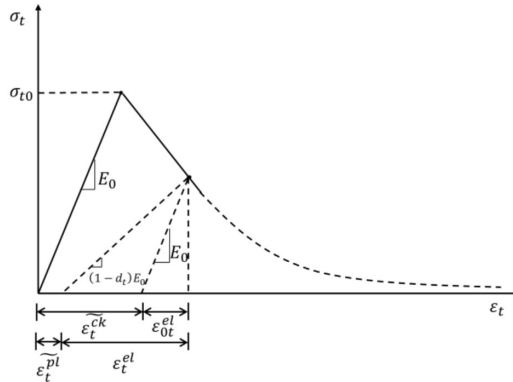


Fig. 3. Stress-strain diagram of concrete under uniaxial tension

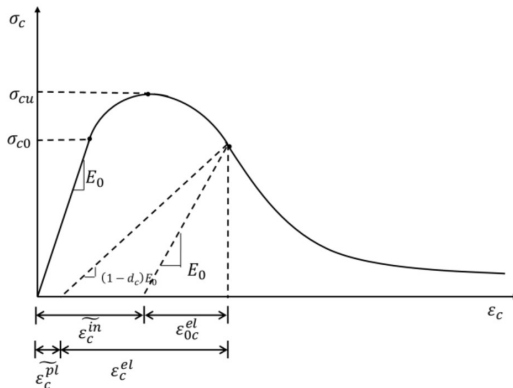


Fig. 4. Stress-strain diagram of concrete under uniaxial compression

The entire range stress-strain relationship under uniaxial tensile and compressive loads is:

$$(3.2) \quad \begin{cases} \sigma_t = (1 - d_t) E_0 (\varepsilon_t - \tilde{\varepsilon}_t^{\text{pl}}) \\ \sigma_c = (1 - d_c) E_0 (\varepsilon_c - \tilde{\varepsilon}_c^{\text{pl}}) \end{cases}$$

where σ_t is the tensile stress of the material, which can be expressed as

$$\frac{\sigma_t}{f_t} = \left[1 + \left(c_1 \frac{w_t}{w_{\text{cr}}} \right)^3 \right] e^{(-c_2 \frac{w_t}{w_{\text{cr}}})} - \frac{w_t}{w_{\text{cr}}} (1 + c_1^3) e^{-c_2}, \quad w_{\text{cr}} = 5.14 \frac{G_F}{f_t}, \quad \sigma_c \text{ is the com-}$$

pressive stress of the material, which can be expressed as $\sigma_c = \frac{f_{c0} x r}{r - 1 + x^r}$, $x = \frac{\varepsilon}{\varepsilon_{c0}}$,

$r = \frac{E_c}{E_c - f_{c0}/\varepsilon_{c0}}$, $\varepsilon_{c0} = 9.37 \times 10^{-4} f_{c0}^{0.25}$. $\tilde{\varepsilon}_t^{\text{pl}}$ is the tensile equivalent plastic strain, and $\tilde{\varepsilon}_c^{\text{pl}}$ is the compressive equivalent plastic strain.

In the plastic damage model of concrete, the uniaxial tensile stress-strain relationship beyond the elastic range is output as $\sigma_t - \widetilde{\varepsilon}_t^{\text{ck}}$, and $\widetilde{\varepsilon}_t^{\text{ck}}$ is the cracking strain, which is the total tensile strain minus the elastic strain of the material without damage, that is:

$$(3.3) \quad \widetilde{\varepsilon}_t^{\text{ck}} = \varepsilon_t - \varepsilon_{0t}^{\text{el}}$$

$$(3.4) \quad \varepsilon_{0t}^{\text{el}} = \frac{\sigma_t}{E_0}$$

Combining formulas (3.2), (3.3), and (3.4):

$$(3.5) \quad \widetilde{\varepsilon}_t^{\text{ck}} = \widetilde{\varepsilon}_t^{\text{pl}} + \frac{d_t \sigma_t}{(1 - d_c) E_0}$$

The uniaxial compressive stress-strain relationship of concrete beyond the elastic range is output as $\sigma_c - \widetilde{\varepsilon}_c^{\text{in}}$, and $\widetilde{\varepsilon}_c^{\text{in}}$ is an inelastic strain, which is the total compressive strain minus the elastic strain of the material without damage, that is:

$$(3.6) \quad \widetilde{\varepsilon}_c^{\text{in}} = \varepsilon_c - \varepsilon_{0c}^{\text{el}}$$

$$(3.7) \quad \varepsilon_{0c}^{\text{el}} = \frac{\sigma_c}{E_0}$$

Combining formula (3.2), formula (3.6), and formula (3.7):

$$(3.8) \quad \widetilde{\varepsilon}_c^{\text{in}} = \widetilde{\varepsilon}_c^{\text{pl}} + \frac{d_c \sigma_c}{(1 - d_c) E_0}$$

The China concrete structure design code [2] is referred to define the tensile and compressive constitutive of concrete above.

3.2. Bond-slip of steel bar to concrete

The interface between steel and concrete is complicated and affected by many factors and it is difficult to get accurate mathematical models of bond strength or bond-slip constitutive relationship based on test results alone. Song [13] conducted concentric pull-out tests of concrete, based on test results, established and verified a complete bond-slip model of reinforced concrete. José [14] presents a new bond element which performs the bond-slip relationship, and verified the accuracy of this new model by test data. Chetra [15] based on the change of the bond-slip between reinforcement and concrete, combined with test analysis, proposed a new steel-concrete bond model on a reinforced concrete shear wall. Peter [16] established two different nonlinear finite element models by the approaches of perfect-bond and bond-slip, compared the results of the two approaches with test results, indicated that both approaches can achieve ideal results. Kang [17] developed an analytical model based on test data and analysed the stress-slip relationship of reinforcement concrete by this model, proved that the model can be used to predict the bond-slip behaviour of reinforcement concrete exactly. As can be seen from the above studies, the current theoretical analysis mode of bonding-slip is basically semi-theoretical and semi-empirical.

ABAQUS numerical finite element analysis software provides a numerical calculation and analysis method for the embedded steel bars, but this method does not consider the bond-slip between steel bars and concrete. For comparing analysis, this study uses those two calculation schemes for comparison. The specific comparative analysis scheme is as follows:

- Scheme A – a separate model that considers the bond-slip between steel bars and concrete;
- Scheme B – an embedded model that does not consider the bond-slip between steel bars and concrete.

The bond-slip constitutive relationship τ_b between steel bars and concrete is the bond-slip curve given in CEB-FIP1990 [18] (3.9), which the constitutive structure is divided into two types: plain steel bar and ribbed steel bar. The bond-slip relationship can be found in Fig. 5.

$$(3.9) \quad \tau_b = \begin{cases} \tau_{\max} (s/s_1)^\alpha, & 0 \leq s \leq s_1 \\ \tau_{\max}, & s_1 \leq s \leq s_2 \\ \tau_{\max} - (\tau_{\max} - \tau_f) \left(\frac{s - s_2}{s_3 - s_2} \right), & s_2 \leq s \leq s_3 \\ \tau_f, & s \geq s_3 \end{cases}$$

For unconstrained and well-bonded concrete components, the relevant parameters in Eq. (3.9) are defined as follows [18]: $\tau_{\max} = 2.0f_{ck}$; $\tau_f = 0.15\tau_{\max}$; $\alpha = 0.4$; s_1 , s_2 , and s_3 are 0.6, 0.6, and 1.0 mm respectively; where f_{ck} is the standard value of compressive strength of concrete cylinder (diameter and height are 150 mm and 300 mm, respectively), when the strength level is less than C50, $f_{ck} = 0.8f_{cu,k}$. In this work, 40 MPa is used for f_{ck} .

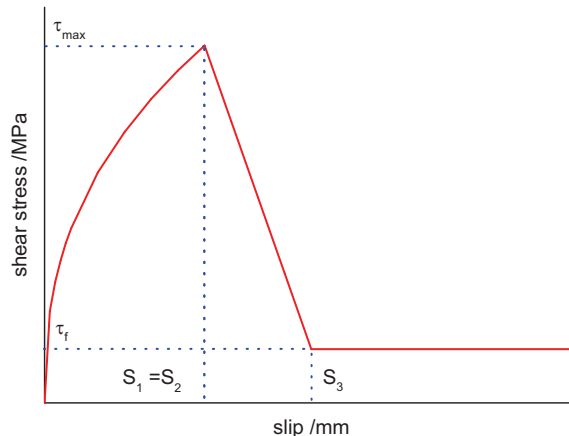


Fig. 5. Bond-slip relationship (cited from [17])

3.3. FEM model

In order to analyze the crack spacing, the FEM model of reinforced concrete needs to be used for simulation and the bond-slip between steel bar and concrete is considered. The crack spacing of the test slab is about 100–300 mm. In order to accurately simulate the crack spacing, the 10 mm element size is used. Considering that the geometry of the hollow slab model is relatively complicated, the research problem in this paper belongs to the stress characteristics of structural details. If a three-dimensional solid element model is used to simulate the beam, the calculation scale will be too large to perform calculations.

After comprehensive consideration, the plane stress model is adopted for calculation. The hollow slab is layered to multiple layers along the height direction, and the thickness of each layer is adjusted according to the size of the hollow slab at the layered height. Table 2 and Figure 6 are for the thickness and width of each layer of the specific plane stress model.

Table 2. Parameters of numerical model (unit: m)

Layer number	Height of each layer	Width of each layer
1–2	0.03	1.03
3–4	0.025	1.03
5	0.0225	0.966
6	0.0225	0.891
7	0.0225	0.863
8	0.0225	0.851
9	0.0225	0.851
10	0.0225	0.863
11	0.0225	0.891
12	0.0225	0.966
13–14	0.0375	1.03
15	0.035	1.03
16–21	0.025	1.03
22	0.02	1.03

Take the 1/2 length of slab for numerical simulation. The longitudinal dimensions of the finite element of concrete and reinforced bars are 10mm, divided into 9154 units in total, the concrete uses CPS4 element, and the reinforced bars use T2D2 element.

The cohesive element of the reinforced concrete in model A uses SPRING2 element. Due to the large number of cohesive elements, 798 springs (399 normal elastic springs for steel bars and 399 longitudinal non-linear springs for steel bars) are automatically added by used ABAQUS python programming [19]. As a comparison, the B model uses the embedded steel bar to establish the connection between steel bar and concrete.

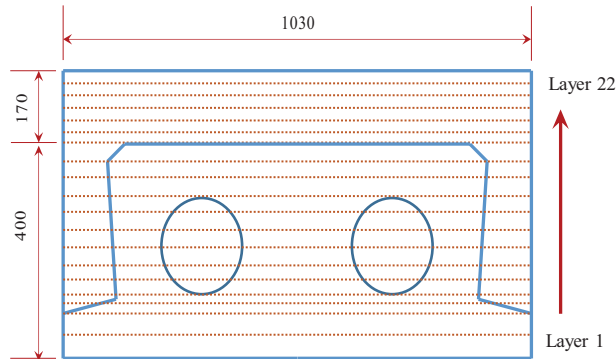


Fig. 6. Hollow slab layering (units: mm)

Figure 7 is the model of a hollow slab element considering the constitutive bond-slip between steel and concrete. In this model: 1) concrete element nodes and reinforced element nodes coincide, 2) add a spring element with a stiffness of 3 to the normal direction, 3) adding nonlinear springs longitudinally. The displacement loading mode is adopted in the numerical model.

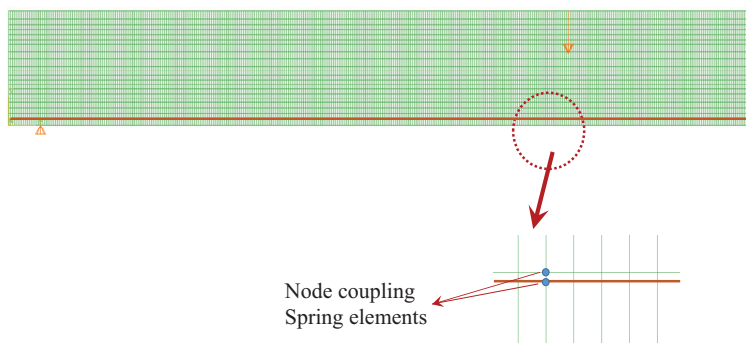


Fig. 7. Finite element model of model A

4. Result analysis

4.1. Load-deflection curve

In order to verify the validity of the numerical model of this study, the results of test and the numerical model with two modeling methods are compared in Figure 8.

It is clearly indicated in Figure 8 that:

- The mid-span load deflection curve of the test and numerical simulation show a typical tri-fold line. The first stage is the elastic stage, the second stage is the concrete cracking stage, and the third stage is the steel yield stage.

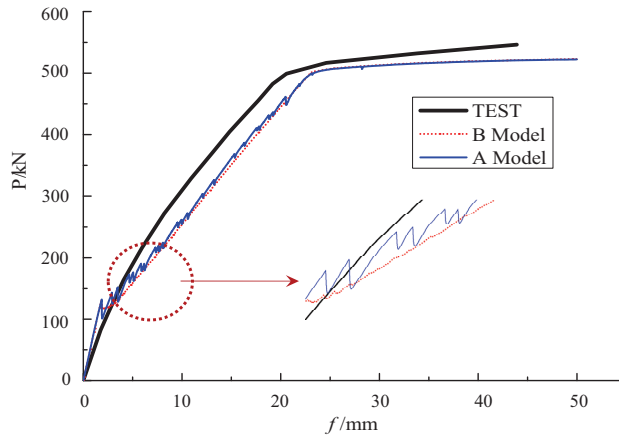


Fig. 8. Load – deflection curves at mid-span

- The cracking load of the test and the numerical model is basically the same. The test result is 115.75 kN while the result of numerical model with different modeling methods are basically the same, about 130.7 kN.
- The yield points of the steel bars in the test and the numerical model are not much different. The test result is 499 kN, the B model is 497.5 kN, and the A model is 503.4 kN.
- The deflection are basically the same of the two models.
- After the steel bar yield, the load deflection curve of the test is slightly strengthened while in the numerical model, the steel bar adopts an ideal elastoplastic model, the load deflection curve remain gentle. The load deflection curve is relatively level in the third section.
- The load deflection curve belongs to the macro-mechanical characteristics of the beam. The bond-slip behavior of reinforced concrete has little effect on the tri-fold line characteristic of the load deflection curve of an 8 m hollow slab beam. That may because the slip of the steel bar to concrete is relative small at the corresponding deflection of the slab.
- Model B adopts embedded steel bar, which does not consider the bond-slip between steel bar and concrete, therefore the load deflection curve after cracking is smooth. For the A model considering the bond-slip relationship of reinforced concrete, the bond-slip constitutive system fails continuously during the crack propagation process, resulting in the instability of the load deflection curve, which is partially jagged.

4.2. Crack spacing analysis

Figure 9 shows the crack spacing during the failure stage of the test, the load at the beginning of this stage is 499 kN.

The cracks spacing at the bottom surface (within a range of 2 m in the mid-span) is 15–30 cm. The reason for this is that the crack spacing is a detailed mechanical properties

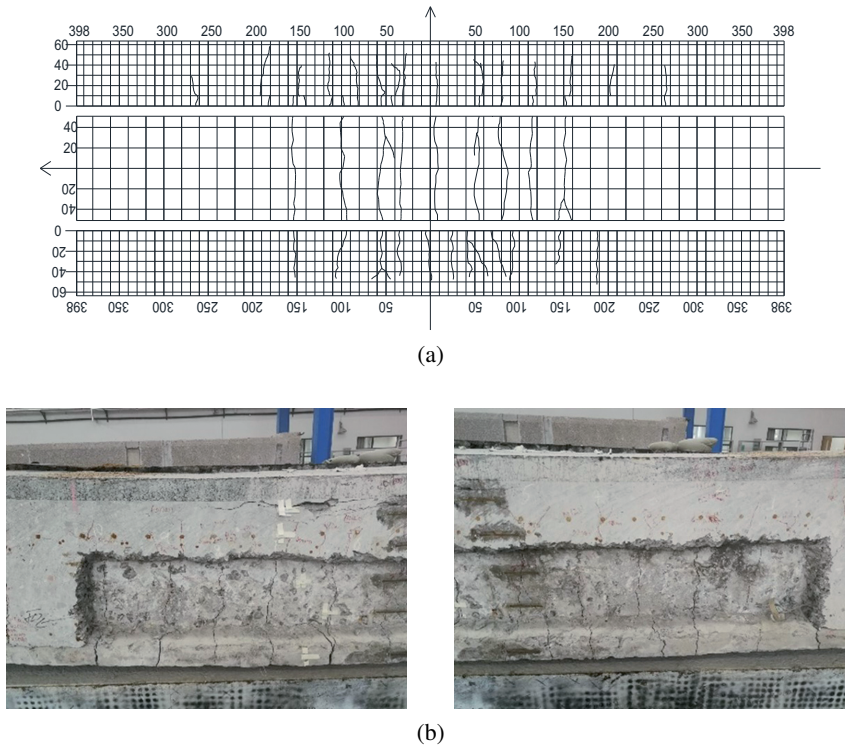


Fig. 9. Crack distribution: (a) Crack sketch (unit cm); (b) Photo of the beam

of reinforced beams and is affected by the tensile strength of the concrete and the bond-slip relationship of the reinforced concrete. Both of the above factors have strong discreteness, which results in a certain randomness when the concrete beam is cracked.

Further analyze the crack spacing of the A/B model under different loadings stage. Considering the checking of cracks is the content of the bridge during normal use, and since the bridge structure may be damaged or overturned in the ultimate state, it is meaningless to check the crack spacing at ultimate state. Therefore, in this study, the crack distribution in the range of 150 kN to 300 kN is analyzed. See Figure 10 for details.

By analyzing Figure 10, the following conclusions can be drawn:

1. Statistics on the crack distribution characteristics of the test beam (Figure 9). There are 6 cracks in the pure bending section. In the numerical model: when the load is 150 kN, there are 7 cracks in the pure bend section of Model A (considering the full-length model); there are 20 cracks in the pure bend section of Model B. Therefore, it can be considered that when numerical simulation is used to study the crack spacing of reinforced concrete beams, the numerical finite element model without considering the bond-slip characteristics cannot accurately predict the distribution characteristics of cracks.

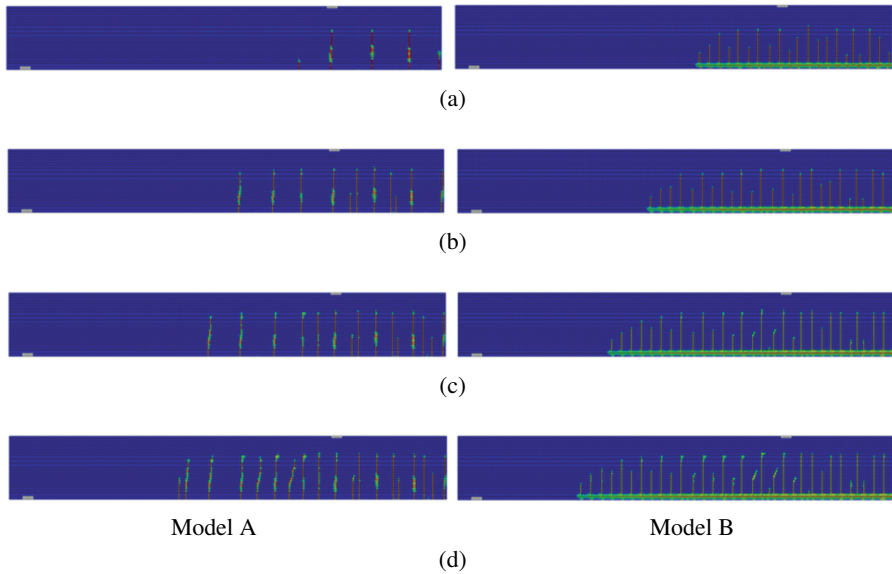


Fig. 10. Crack propagation of Model A and Model B under (a) 150 kN, (b) 200 kN, (c) 250 kN and (d) 300 kN

2. In the model A considering bond-slip, when the flexure crack appeared, the concrete on both sides of the crack did not appear damage. In the B model without considering the bond-slip, when the flexure crack appeared, the concrete in the reinforced layer almost suffered different degrees of damage along the longitudinal direction. By comparing the crack distribution characteristics of the test beam, it can be seen that the numerical finite element model without considering the bond-slip characteristics cannot accurately simulate the stress characteristics of the concrete element adjacent to the reinforcement when the crack occurs.
3. After the main flexure cracks are generated in Model A, a small number of secondary bending cracks appear with the increase of the load; while in Model B, more primary flexure cracks appear in the initial stage of cracking. With the increase of the load, the crack spacing of the A/B model tends to approach under the load of 300 kN.

4.3. Stress distribution in steel bar

The distribution of crack spacing of reinforced concrete is closely related to the bond-slip behavior between steel bar and concrete. After cracking, the concrete stress at the crack is released, and the stress of the steel bar at the crack will increase. This study will further compare the development and distribution of stresses in rebars according to A/B model for different loads after cracking. Similar to the crack spacing analysis, the analysis of stresses in rebars is carried out in the range of loads 150–300 kN (Figure 11).

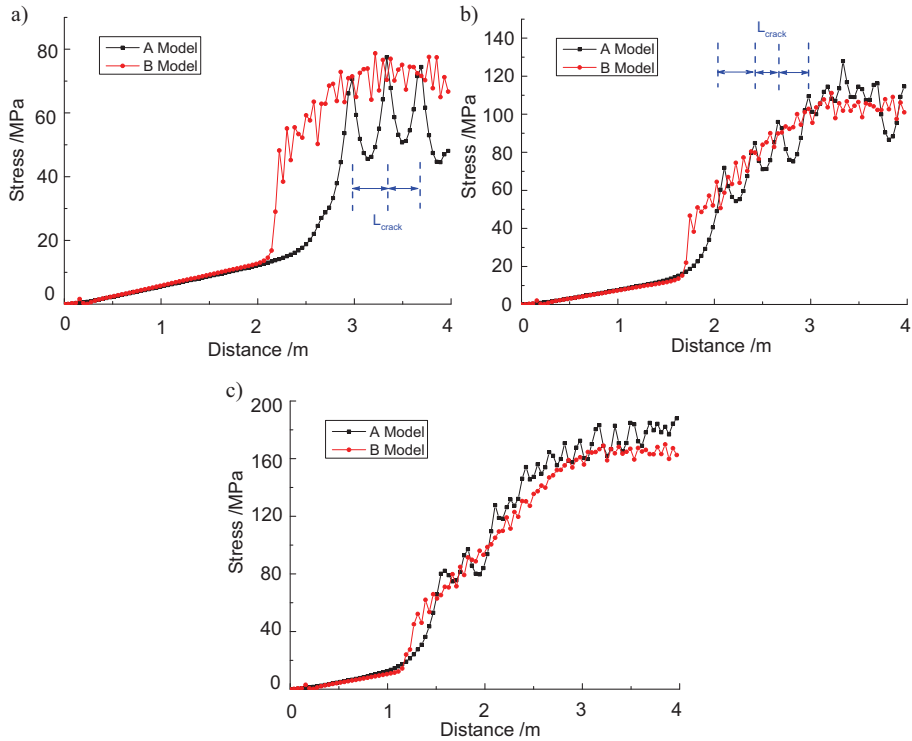


Fig. 11. Stress distribution of reinforcement bars under (a) 150 kN; (b) 200 kN and (c) 300 kN

By analyzing Figure 11, the following conclusions can be drawn:

1. The macro characteristics of the stress distribution characteristics of the A/B model are consistent: they are small near the support and large at the mid-span.
2. When the load is 150 kN, the stress of the steel bar in the pure flexure section of model A has typical wave characteristics, and the distance between the two stress wave peaks is the crack spacing. The stress distribution of the steel bars in the pure flexure section of the B-model shows serrated, and the exact value of the crack spacing cannot be obtained. The reason for this is that the B model does not consider the bond-slip characteristics between steel bar and concrete, which causes damage to the concrete around the reinforcement, and the stress distribution of the reinforcement is also irregular.
3. When the load is 200 kN, the stress distribution of the steel bars in the pure flexure section of model A no longer has a typical wave feature. This feature is translated toward the support, and stress peaks appear within a range of 2 to 3 m from the support. The reason for this is that the secondary flexure cracks appear in the pure flexure section at the load of 200 kN in model A, which results in relatively complicated stress distribution characteristics of the steel bars. The stress distribution of steel bars in model B is also irregular.

4. When the load is 300 kN, the reinforcement stress distribution of the A/B model is irregular. This phenomenon shows that the closer to the failure load of the beam, the more difficult it is to analyze the crack spacing from the stress distribution characteristics of the reinforcement.

5. Conclusions

The load deflection curve belongs to the macro-mechanical characteristics of the beam. The bond-slip characteristics of reinforced concrete have little effect on the three-fold characteristic of the load deflection curve of an 8 m hollow slab beam by comparing with the test.

Without considering the bond-slip of reinforced concrete, the load deflection curve after cracking is smooth. For the model considering the bond-slip relationship of reinforced concrete, due to the influence of the bond-slip relationship of reinforced concrete, the load deflection curve is partially serrated. The test load-deflection curve does not readily represent this serrate phenomenon.

When using numerical simulation to analyze flexure cracks, in the numerical model that does not take into account the characteristics of bond-slip, almost all of the concrete in the reinforced layer is damaged in the longitudinal direction, and the distribution characteristics of the cracks cannot be accurately determined.

Regardless of whether bond-slip is considered or not, the macroscopic characteristics of the stress distribution characteristics of the reinforcement are consistent: they are small near the support and large at the mid-span.

In the initial of cracking, the model considering the bond-slip characteristics can calculate the crack spacing based on the stress distribution characteristics of the reinforcement. However, with the expansion of secondary flexure cracks, in the later stage of cracking, the models with and without considering the bond-slip characteristics cannot calculate the crack spacing based on the stress distribution characteristics of the reinforcement.

The effect of prestress on deflection and crack layout in a hollow slab bridge will be studied in future work.

Acknowledgements

This work is financially supported by the Transportation Science and Technology Projects of Shandong Province, China (No. 2021B62).

References

- [1] JTG 3362-2018 Specification for design of highway reinforced concrete and prestressed concrete bridges and culverts. Beijing, China, 2018.
- [2] GB50010-2010 Code for design of concrete structures. Beijing, China, 2015.

- [3] A. Lindorf, R. Lemnitzer, and M. Curbach, "Experimental investigations on bond behaviour of reinforced concrete under transverse tension and repeated loading", *Journal of Engineering Structures*, vol. 31, no. 7, pp. 1469–1476, 2009, doi: [10.1016/j.engstruct.2009.02.025](https://doi.org/10.1016/j.engstruct.2009.02.025).
- [4] R. Piyasena, Y.C. Loo, and S. Fragomeni, "Factors influencing spacing and width of cracks in reinforced concrete; new prediction formulae", *Journal of Advanced Structural Engineering*, vol. 7, no. 1, pp. 49–60, 2004, doi: [10.1260/136943304322985756](https://doi.org/10.1260/136943304322985756).
- [5] G. Creazza and S. Russo, "A new model for predicting crack width with different percentages of reinforcement and concrete strength classes", *Journal of Materials and Structures*, vol. 32, pp. 520–524, 1999, doi: [10.1007/BF02481636](https://doi.org/10.1007/BF02481636).
- [6] B.H. Oh and S.H. Kim, "Advanced crack width analysis of reinforced concrete beams under repeated loads", *Journal of Structural Engineering*, vol. 133, no. 3, pp. 411–420, 2007, doi: [10.1061/\(ASCE\)0733-9445\(2007\)133:3\(411\)](https://doi.org/10.1061/(ASCE)0733-9445(2007)133:3(411)).
- [7] H.G. Kwak and J.Y. Song, "Cracking analysis of RC members using polynomial strain distribution function", *Journal of Engineering Structures*, vol. 24, no. 4, pp. 455–468, 2002, doi: [10.1016/S0141-0296\(01\)00112-2](https://doi.org/10.1016/S0141-0296(01)00112-2).
- [8] EN1992-1-1 Design of concrete structures-general rules and rules for building. European Committee for Standardization, 2004.
- [9] J.J. Jiang, *Concrete structure engineering*. Beijing, China: China Construction Industry Press, 1998.
- [10] A. Casanova, L. Jason, and L. Davenne, "Bond slip model for the simulation of reinforced concrete structures", *Journal of Engineering Structures*, vol. 39, pp. 66–78, 2012, doi: [10.1016/j.engstruct.2012.02.007](https://doi.org/10.1016/j.engstruct.2012.02.007).
- [11] E. Giner, et al., "An Abaqus implementation of the extended finite element method", *Journal of Engineering Fracture Mechanics*, vol. 76, no. 3, pp. 347–368, 2009, doi: [10.1016/j.engfracmech.2008.10.015](https://doi.org/10.1016/j.engfracmech.2008.10.015).
- [12] Abaqus, *Abaqus Analysis User's Manual, version 2021*.
- [13] X. Song, Y. Wu, X. Gu, and C. Chen, "Bond behaviour of reinforcing steel bars in early age concrete", *Journal of Construction and Building Materials*, vol. 94, pp. 209–217, 2015, doi: [10.1016/j.conbuildmat.2015.06.060](https://doi.org/10.1016/j.conbuildmat.2015.06.060).
- [14] J. Santos and A. A. Henriques, "New finite element to model bond–slip with steel strain effect for the analysis of reinforced concrete structures", *Journal of Engineering Structures*, vol. 86, pp. 72–83, 2015, doi: [10.1016/j.engstruct.2014.12.036](https://doi.org/10.1016/j.engstruct.2014.12.036).
- [15] C. Mang, L. Jason, and L. Davenne, "Crack opening estimate in reinforced concrete walls using a steel–concrete bond model", *Archives of Civil and Mechanical Engineering*, vol. 16, no. 3, pp. 422–436, 2016, doi: [10.1016/j.acme.2016.02.001](https://doi.org/10.1016/j.acme.2016.02.001).
- [16] P. Grassl, M. Johansson, and J. Leppanen, "On the numerical modelling of bond for the failure analysis of reinforced concrete", *Journal of Engineering Fracture Mechanics*, vol. 189, pp. 13–26, 2018, doi: [10.1016/j.engfracmech.2017.10.008](https://doi.org/10.1016/j.engfracmech.2017.10.008).
- [17] S. Kang, S. Wang, X. Long, D. Wang, and C. Wang, "Investigation of dynamic bond-slip behaviour of reinforcing bars in concrete", *Journal of Construction and Building Materials*, vol. 262, art. no. 120824, 2020, doi: [10.1016/j.conbuildmat.2020.120824](https://doi.org/10.1016/j.conbuildmat.2020.120824).
- [18] CEB-FIP, *CEB-FIP Model Code 90*. London: Thomas Telford Ltd., 1993.
- [19] F. Zhang, X. F. Xu, and S. C. Li, "Bond-slip model for HB-FRP systems bonded to concrete", *China Journal of Highway and Transport*, vol. 28, pp. 38–44, 53, 2015, doi: [10.19721/j.cnki.1001-7372.2015.01.006](https://doi.org/10.19721/j.cnki.1001-7372.2015.01.006).